# Fluoride Removal from Water by Adsorption on a High Alumina Content Bauxite

Roberto Lavecchia*, Franco Medici, Luigi Piga, Gilberto Rinaldi, Antonio Zuorro

Dipartimento di Ingegneria Chimica, Materiali e Ambiente, Università "La Sapienza",
Via Eudossiana 18, 00184 Roma, Italy
roberto.lavecchia@uniroma1.it

Drinking water contamination by fluoride is recognized as a major public health problem in many parts of the world. In fact, although fluoride is an essential trace element for animals and humans, excessive fluoride intake may cause adverse health effects.

In this study we investigated the potential of a natural, high alumina content, bauxite for the removal of fluoride from contaminated water. Both batch and continuous experiments were performed. In continuous-flow column experiments, the effects of inlet fluoride concentration (5–50 mg L$^{-1}$) and flow rate (up to 2.5 mL min$^{-1}$) on breakthrough time and adsorption capacity were studied. Batch equilibrium data were found to be well described by the Freundlich equation. Column studies showed that the dynamic adsorption capacity of the bed decreased as the inlet fluoride concentration and the flow rate increased. A maximum fluoride uptake capacity of 3.125 mg g$^{-1}$ was determined. Overall, the results obtained indicate that this bauxite could be effectively used for defluoridation of drinking water.

## 1. Introduction

Fluoride is considered an essential element for animals and humans because of the role it plays in bone and dentin mineralization (Grynpas et al., 2000). The beneficial effects of fluoride are mainly attributed to its ability to stimulate osteoblast activity and to reinforce tooth enamel when incorporated into hydroxyapatite structures (Caverzasio et al., 1998). However, these effects occur only over a relatively narrow range of fluoride concentrations and disappear or are reversed at higher doses. Excessive fluoride exposure may cause irreversible demineralization of bone and tooth tissues, a condition known as fluorosis, and long-term damage to the brain, liver, thyroid and kidney (Barbier et al., 2010; Gazzano et al., 2010).

The majority of fluoride intake is from drinking water. According to current knowledge, a fluoride concentration of about 0.5 mg L$^{-1}$ is beneficial in preventing dental caries during tooth development, while levels higher than 1.5 g L$^{-1}$ may result in fluorosis or other health problems (Dean, 2006). In regions where fluoride occurs naturally, the US Environmental Protection Agency (EPA) prescribes a maximum level of fluoride in drinking water at 4 mg L$^{-1}$, a value that is considered adequate for the prevention of skeletal fluorosis (EPA, 2006). A secondary maximum contaminant level of 2 mg L$^{-1}$ is recommended to minimize the "cosmetic" risk of dental fluorosis, which can occur when fluoride is incorporated into enamel (NRC, 2006). The World Health Organization (WHO) guidelines suggest optimum levels of fluoride concentration at 1 and 1.2 mg L$^{-1}$ for warmer and cooler climates, respectively (WHO, 2004). The difference is due to greater water consumption in warmer climates. In most European countries, including Italy, the maximum level of fluoride in drinking water is 1.5 mg L$^{-1}$.

In Italy, however, more than 100 districts of two regions (Lazio and Toscana) exceed the allowable levels. Similar, or even more critical, situations are found in other European and non-European countries (Spencer and Do, 2008). In India alone it is estimated that more than 6 million people are seriously affected by fluorosis and another 62 million are exposed to it (Mariappan et al., 2000).

For the above reasons, much attention has been devoted in recent years to developing effective and economical methods for defluoridation of drinking water. Conventional treatments include chemical precipitation, adsorption, ion exchange, reverse osmosis and electrodialysis. Among them, adsorption is considered to be a viable approach due to its simplicity and cost-effectiveness. A wide variety of adsorbents, including fly ash (Chaturvedi et al., 1990), limestone (Nair et al., 1994), clay minerals (Srimurali et al., 1998), rare earth oxides (Raichur and Basu, 2001), alumina (Ku and Chiou, 2002; Ghorai and Pant, 2005), bone char (Leyva-Ramos et al., 2010) and many others have been studied for this purpose.

The present study was aimed at assessing the potential of a high alumina content bauxite to remove fluoride from contaminated water. Bauxite is an abundantly available material consisting of aluminum oxides with minor and variable amounts of silica, iron oxides, titanium oxide and alumina silicate clays. Heat-activated bauxite has been extensively investigated for the removal of pollutants such as arsenic (Altundogan et al., 2002), chromium (Erden et al., 2004) and fluoride (Sujana and Anand, 2010) from water. In contrast, very few studies have been devoted to the use of untreated bauxite and, consequently, little is known about its suitability for fluoride removal.

## 2. Experimental

### 2.1 Materials

Sodium fluoride (CAS No. 7681-49-4) with purity > 99 % was purchased from Merck (Darmstadt, Germany). All other chemicals were analytical grade and used without further purification. Synthetic fluoride solutions were prepared by adding appropriate amounts of sodium fluoride to distilled water.

Bauxite was obtained from a deposit in Texas (USA), hematite and vermiculite were from Elba (Livorno, Italy), lava from Stromboli (Messina, Italy) and black pozzolana from Lunghezza (Roma, Italy).

### 2.2 Methods

The sorption materials were preliminary ground and sieved to obtain powders below 1.18 mm of diameter. After careful washing with deionized water, the materials were dried at 110 °C in an electric oven for 3 h. Then they were cooled in air to room temperature and characterized by standard analytical methods and by X-ray diffraction.

To assess the ability of each adsorbent to remove fluoride from water, preliminary batch screening tests were conducted. One g of powdered sample was contacted with 100 mL of 10 mg $L^{-1}$ fluoride solution for 1 h under gentle agitation. After this time, a sample of liquid was taken and the residual fluoride concentration was measured. A similar procedure was used to perform equilibrium experiments. In these experiments the liquid-to-solid ratio was set at 100 mL $g^{-1}$ and the initial fluoride concentration was varied between 5 and 100 mg $L^{-1}$.

Column studies were carried out in a glass column with an inner diameter of 1 cm and a length of 30 cm. A glass-wool plug was placed in the bottom of the column to support the adsorbent bed and prevent the outflow of particles. The amount of adsorbent was fixed at 4 g (corresponding to a bed height of 5.5 cm), the inlet fluoride concentration was varied from 5 to 50 mg $L^{-1}$ and the flow rate from 0.5 to 2.5 $cm^3$ $min^{-1}$. Samples of the outlet solution were collected at definite time intervals and analysed for fluoride content.

Batch and column experiments were performed at pH 7.0 ± 0.1 and room temperature (20 ± 2 °C). The concentration of fluoride in the aqueous solution was determined by a potentiometer equipped with an ion-selective electrode (DC219-F, Mettler–Toledo, Novate Milanese, Italy). A series of standard fluoride solutions with concentrations ranging from 0.1 to 10 mg $L^{-1}$ was used to construct the calibration curve.

## 3. Results and discussion

### 3.1 Preliminary screening tests

Batch screening tests gave the results presented in Table 1, from which it can be seen that percent removal of fluoride ranged from 7.3 % (hematite) to 38.5 % (bauxite). Because of its significantly higher efficiency, bauxite was used in subsequent experiments. Chemical analysis by standard gravimetric methods showed that $Al_2O_3$ (81.5 %), $Fe_2O_3$ (9.3 %) and $SiO_2$ (8.9 %) were the main bauxite constituents. No heavy metals (Pb, Cd, As, Cr) were detected. XRD analysis revealed the presence of hematite [$Fe_2O_3$], gibbsite [Al(OH)$_3$)] and anatase [$TiO_2$] as the main phases.

### 3.2 Equilibrium studies

The time needed to reach equilibrium was of the order of 3 h and independent of the initial fluoride concentration (Figure 1). The equilibrium concentrations in the liquid ($c^*$) were determined after this time, while the concentrations in the adsorbed phase ($q^*$) were calculated as:

$$q^* = \frac{V_L}{w}(c_0 - c^*) \tag{1}$$

where $V_L$ is the volume of the aqueous solution, $w$ is the mass of adsorbent and $c_0$ is the initial fluoride concentration. The data so obtained were well described by the two-parameter Freundlich equation:

$$q^* = K_F(c^*)^{1/n} \tag{2}$$

where $K_F$ is the Freundlich constant and $1/n$ is the heterogeneity factor. $K_F$ represents the amount of solute adsorbed at an equilibrium concentration of unity and thus is a measure of the adsorption capacity of the material, while $n$ reflects the adsorption intensity. It is generally stated that values of $n$ in the range 2–10, 1–2 and <1 indicate, respectively, good, moderate and poor adsorption characteristics. The Freundlich parameters were obtained from the slope and intercept of the log–log plot shown in Figure 2, which yielded $K_F = 0.957$ mg$^{1-1/n}$ g$^{-1}$ L$^{1/n}$ and $n = 3.18$. The maximum adsorption capacity under the conditions tested was 3.15 mg g$^{-1}$.

*Table 1: Results of preliminary screening tests. FR is the percent fluoride removal*

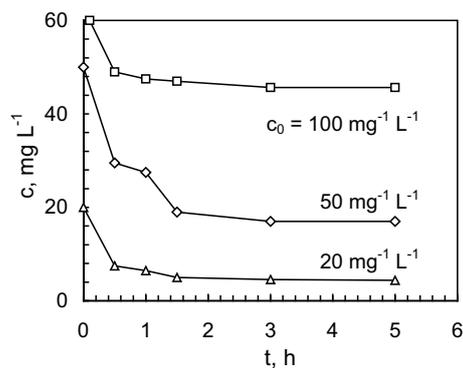| Material | Origin | FR (%) |
|---|---|---|
| Bauxite | Texas (USA) | 38.5 |
| Hematite | Elba (Italy) | 7.3 |
| Lava | Stromboli (Italy) | 10.0 |
| Black pozzolana | Lunghezza (Italy) | 15.0 |
| Vermiculite | Elba (Italy) | 13.0 |



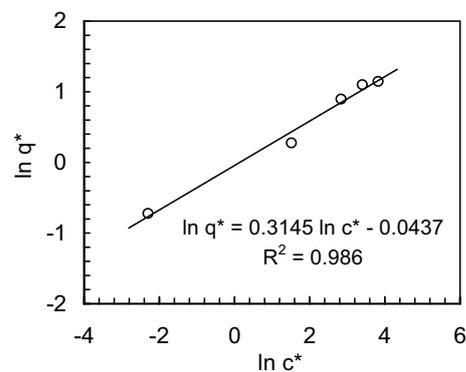*Figure 1: Fluoride concentration decay curves*



*Figure 2: Freundlich plot for fluoride adsorption*

Based on these results, it can therefore be inferred that fluoride is effectively adsorbed on bauxite and that the Freundlich model provides a satisfactory description of the adsorption equilibrium. Similar conclusions were drawn from studies on fluoride removal by different adsorbents such as activated alumina (Ghorai and Pant, 2005), hydroxyapatite (Wang et al., 2011), brushite (Mourabet et al., 2011) and zirconium-iron oxide (Dou et al., 2011).

### 3.3 Column studies

Column experiments were carried out at different inlet fluoride concentration and flow rate. The results, expressed as the ratio between outlet and inlet fluoride concentration ($c/c_0$) versus time, gave typical S-shaped breakthrough curves (Figure 3). As the flow rate ($F$) increased, the curves became steeper and the breakpoint time decreased. Moreover, much sharper curves were observed at higher inlet fluoride concentration. The area above the breakthrough curve (up to $c/c_0$ = 1) provides a measure of the amount of adsorbed fluoride per unit weight of adsorbent, the so-called dynamic adsorption capacity. This quantity decreased as the inlet fluoride concentration and the flow rate in the column were increased.

Breakthrough curves were analysed by determining the following parameters: the breakthrough time ($t_B$), i.e., the time corresponding to $c/c_0$ = 0.5; the adsorbent capacity at the breakthrough point ($BPC$), i.e., the specific amount of fluoride adsorbed at $t_{0.5}$ and the adsorbent capacity at the exhaustion point ($EPC$), i.e., the specific amount of fluoride adsorbed at exhaustion. $BPC$ and $EPC$ were calculated as:

$$BPC = \frac{c_0 V_B}{w} \quad ; \quad EPC = \frac{c_0 V_E}{w} \tag{3}$$

where $V_B$ and $V_E$ are the volumes of solution treated at, respectively, the breakthrough point and the exhaustion point. The results are presented in Table 2.
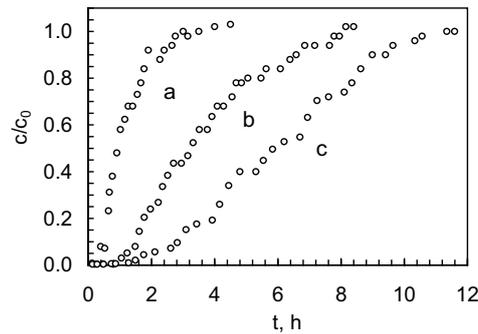


Figure 3: Breakthrough curves for fluoride removal ($c_0$ = 25 g $L^{-1}$) at different fluow rates: a = 2.5 cm$^3$ min$^{-1}$; b = 1 cm$^3$ min$^{-1}$; c = 0.5 cm$^3$ min$^{-1}$

Table 2: Characteristic column adsorption parameters calculated from the breakthrough curves

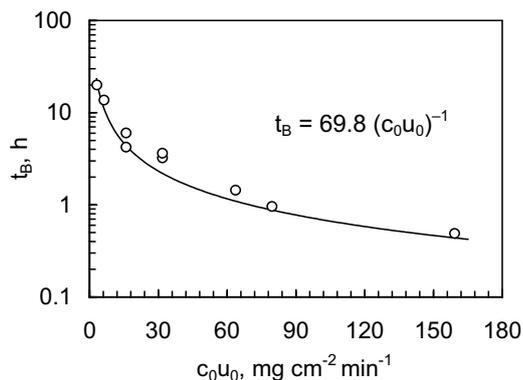| $c_0$ (mg $L^{-1}$) | $F$ (cm$^3$ min$^{-1}$) | $t_B$ (h) | $BPC$ (mg g$^{-1}$) | $EPC$ (mg g$^{-1}$) |
|---|---|---|---|---|
| 5 | 0.5 | 20.00 | 1.075 | >1.500 |
|  | 1.0 | 13.67 | 1.025 | >1.500 |
|  | 2.5 | 4.22 | 0.775 | >1.500 |
| 25 | 0.5 | 6.02 | 1.244 | 2.406 |
|  | 1.0 | 3.23 | 1.206 | 2.938 |
|  | 2.5 | 0.96 | 1.063 | 3.125 |
| 50 | 0.5 | 3.62 | 1.788 | 2.888 |
|  | 1.0 | 1.44 | 1.438 | 2.613 |
|  | 2.5 | 0.49 | 0.938 | 1.375 |

$$t_B = 69.8 \, (c_0 u_0)^{-1}$$

*Figure 4: Experimental and calculated (eqn. 4) breakthrough times for fluoride removal in column tests*

Examination of the data reveals that the breakthrough time decreased with increasing flow rate and inlet fluoride concentration. There were also some effects on *BPC* and *EPC*, which assumed mean values of, respectively, 1.172 (± 0.298) and 2.557 (± 0.632) mg g$^{-1}$.

Interestingly, the largest value of fluoride uptake capacity at exhaustion (*EPC* = 3.125 mg g$^{-1}$) was very close to the maximum adsorption capacity at equilibrium (3.15 mg g$^{-1}$). This suggests that a fluoride-saturated zone is formed in the bauxite bed whose extension increases with increasing fluoride uptake until the entire bed volume is covered. The values of $t_B$ were correlated with inlet fluoride concentration ($c_0$) and flow rate (*F*) by the relation developed by Hutchins (1973) from the Bohart and Adams model:

$$t_B = \frac{N_0}{c_0 u_0}(Z - Z_0) \tag{4}$$

where $N_0$ is the column adsorption capacity, $u_0$ is the superficial liquid velocity based on empty column ($u_0 = F/A_C$), $Z$ is the bed height and $Z_0$ is the length of the dynamic bed mass-transfer zone, which is equivalent to the adsorption front where the adsorbent material is partly saturated with fluoride. As apparent from Figure 4, very good agreement was found between the experimental and calculated breakthrough times, indicating that eqn. (4) is appropriate to describe the effects of fluoride concentration and liquid flow rate on the column behavior. Since $N_0$ and $Z_0$ depend on both transport phenomena and equilibrium conditions, it may be expected that they vary with liquid flow rate and fluoride concentration (Hamdaoui, 2006). While the available data do not allow us to estimate them separately, it is evident from eqn. 4 that an increase in the thickness of the mass-transfer zone and, consequently, in the adsorption capacity of the bed should occur in such a way as to keep the product $N_0 (Z - Z_0)$ constant.

Referring to the maximum uptake capacity, we note that the value found in this study (3.125 mg g$^{-1}$) is higher than that of 1.45 mg g$^{-1}$ reported for fluoride removal by activated alumina (Ghorai and Pant, 2004) and is comparable with the values determined using activated carbon and aligned carbon nanotubes, a new class of adsorbents (Li et al., 2003). This clearly supports the use of this bauxite for the treatment of drinking water with high fluoride content (typically 5 to 20 mg L$^{-1}$).

## 4. Conclusions

The high alumina content bauxite examined in this study showed promising properties as a low-cost and effective adsorbent for the removal of fluoride from water. Bauxite is an abundantly available material and, according to the results presented here, could be used without being preliminarily activated as, instead, is required for alumina and other adsorbents.

Future research should include assessment of adsorbent regeneration, process optimization and a detailed cost-benefit analysis.

## References

Altundogan H.S., Altundogan S., Tümen F., Bildik M., 2002, Arsenic adsorption from aqueous solutions by activated red mud, Waste Manag. 22, 357–363.

Barbier O., Arreola-Mendoza L., Del Razo L.M., 2010, Molecular mechanisms of fluoride toxicity, Chem. Biol. Interact., 188, 319–333.

Caverzasio J., Palmer G., Bonjour J.P., 1998, Fluoride: Mode of Action, Bone, 22, 585–589.

Chaturvedi A.K., Yadava K., Pathak K.C., Singh V.N., 1990, Defluoridation of water by adsorption on fly ash, Water Air Soil Pollut., 49, 51–61.

Dean H.T., 2006, Endemic fluorosis and its relation to dental caries, Public Health Rep., 121, 213–219.

Dou X., Zhang Y., Wang H., Wang T., Wang Y., 2011, Performance of granular zirconium–iron oxide in the removal of fluoride from drinking water, Water Res., 45, 3571–3578.

EPA (US Environmental Protection Agency), 2006, Drinking water contaminants: Consumer factsheets <www.epa.gov/safewater/contaminants> Accessed 30.11.2011.

Erden M., Altundogan H.S., Turner F., 2004, Removal of hexavalent chromium by using heat-activated bauxite, Minerals Eng., 17, 1045–1052.

Gazzano E., Bergandi L., Riganti C., Aldieri E., Doublier S., Costamagna C., Bosia A., Ghigo D., 2010, Fluoride effects: the two faces of Janus, Curr. Med. Chem., 17, 2431–2441.

Ghorai S., Pant K.K., 2004, Investigations on the column performance of fluoride adsorption by activated alumina in a fixed-bed, Chem. Eng. J., 98, 165–173.

Ghorai S., Pant K.K., 2005, Equilibrium, kinetics and breakthrough studies for adsorption of fluoride on activated alumina, Sep. Purif. Technol., 42, 265–271.

Grynpas M.D., Chachra D., Limeback H., 2000, The Action of Fluoride on Bone, The Osteoporosis Primer. Eds. Henderson J.E., Goltzman D., Cambridge University Press, Cambridge, UK.

Hamdaoui O., 2006. Dynamic sorption of methylene blue by cedar sawdust and crushed brick in fixed bed columns, J. Hazard. Mater., B138, 293–303.

Hutchins R.A., 1973, New method simplifies design of activated carbon systems, Chemical Engineering, 80, 133–135.

Ku Y., Chiou H.M., 2002, The adsorption of fluoride ion from aqueous solution by activated alumina, Water Air Soil Poll., 133, 349–361.

Leyva-Ramos R., Rivera-Utrilla J., Medellin-Castillo N.A., Sanchez-Polo M., 2010, Kinetic modeling of fluoride adsorption from aqueous solution onto bone char, Chem. Eng. J., 158, 458–467.

Li Y.H., Wang S., Wei J., Zhang X., Wei J., Xu C., Luan Z., Wu D., 2003, Adsorption of fluoride from water by aligned carbon nanotubes, Mater. Res. Bull., 38, 469–476.

Mariappan P., Yegnaraman V., Vasudevan T., 2000, Occurrence and removal possibilities of fluoride in groundwaters of India, Pollut. Res., 19, 165–177.

Mourabet M., El Boujaady H., El Rhilassi A., Ramdane H., Bennani-Ziatni M., El Hamri R., Taitai A., 2011, Defluoridation of water using brushite, Desalination, 278, 1–9.

Nair S., Jallan G., Pandey G.S, 1994, Studies on fluoride removal by limestone, Fluoride, 23, 35–36.

NRC (National Research Council), 2006, Fluoride in Drinking Water: A Scientific Review of EPA's Standards. The National Academies Press, Washington, DC, USA.

Raichur A.M., Basu M.J., 2001, Adsorption of fluoride onto mixed rare earth oxides, Sep. Purif. Tech., 24, 121–127.

Spencer A., Do L., 2008, Changing risk factors for fluorosis among South Australian children, Community Dentist. Oral Epidemiol., 36, 210–218.

Srimurali M., Pragati A., Karthikeyan J., 1998, A study on removal of fluorides from drinking water by adsorption on to low cost materials, Environ. Poll., 99, 285–289.

Sujana M.G., Anand, S., 2010, Fluoride removal studies from contaminated ground water by using bauxite, Desalination, 267, 222–227.

Wang Y., Chen N., Wei W., Cui J., Wei Z., 2011, Enhanced adsorption of fluoride from aqueous solution onto nanosized hydroxyapatite by low-molecular-weight organic acids, Desalination, 276, 161–168.

WHO (World Health Organization), 2004, Guidilines for drinking-water contaminants <www.who.int/water_sanitation_health/dwq/nutfluoride.pdf> Accessed 30.11.2011.